

# Numerical computation of dispersion relations for multi-layered anisotropic structures

N.D. Botkin, K.-H. Hoffmann, O.A. Pykhiteev and V.L. Turova

Ludwig-Erhard-Allee 2, 53175 Bonn, Germany, e-mail: pykhiteev@caesar.de

## ABSTRACT

The paper presents an algorithm and a program for the computation of the velocity of acoustic waves excited in anisotropic multi-layered structures. The investigation is motivated by modelling of a biosensor which serves for the detection and quantitative measurement of microscopic amounts of biological substances. The program is supplied with a user friendly graphical interface and can be useful for researchers working on acoustic sensors.

**Keywords:** dispersion relations, surface acoustic waves, multi-layered structures, linear elasticity

## 1 INTRODUCTION

The paper outlines an algorithm and a program for the computation of the velocity of acoustic waves excited in anisotropic multi-layered structures. In contrast to acoustic waves in bulk materials, the wave velocity in laminate structures depends on the frequency because of the interaction between the layers with different acoustic properties. Therefore, one can speak about dispersion relations that express the connection between the velocity and the frequency of acoustic waves.

The investigation of dispersion relations is motivated by the modelling of a biosensor [1] that serves for the detection and quantitative measurement of microscopic amounts of biological substances. The operating principle of the biosensor is based on the generation and detection of horizontally polarized shear Love waves. From the mechanical point of view, the biosensor is a multi-layered structure consisting both of isotropic and anisotropic layers. The biological substance adheres to the surface of the top layer so that a new layer is being formed, which changes the velocity of shear waves propagating along the sensors surface. Thus, an effective tool for computing the velocity of waves in multi-layered structures would enable us to estimate the sensitivity of the biosensor in dependance on its constructive features and operation parameters.

Classical examples of the derivation of dispersion relations demonstrate that the problem is solvable analytically in simplest cases only (see e.g. [2]). Therefore, it is reasonable to examine semi-analytical meth-

ods that use both analytical representations of solutions and numerical determination of their parameters. Such a method and the related program are developed by the authors. The algorithm is based on the construction of travelling wave solutions of elasticity equations describing deformations in the layers. The wave velocity is computed from the fitting of mechanical conditions on the interfaces between the layers. These conditions express the continuity of the displacement field and the pressure equilibrium for each pair of the layers. Feasible wave velocities are the roots of a non-negative real function (fitting function) that expresses a measure of the inconsistency in the interface conditions.

## 2 MATHEMATICAL MODEL

### 2.1 Simple structure

First, consider a simplified structure shown in Figure 1. Here, an anisotropic layer lies on an anisotropic half-space substrate. The fluid is not present in the model. The computation of the velocity of surface acoustic waves is based on the construction of travelling wave solutions that exponentially decrease with  $x_3$ .

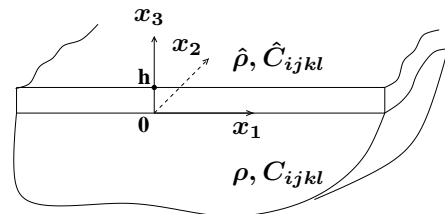


Figure 1: A sample structure. Here,  $\hat{\rho}$ ,  $\rho$ , and  $\hat{C}_{ijkl}$ ,  $C_{ijkl}$  are the densities and the elastic stiffness tensors, respectively

The elasticity equations for the substrate and the top layer read:

$$\rho u_{itt} - C_{ijkl} \frac{\partial^2 u_l}{\partial x_j \partial x_k} = 0, \quad i = 1, 2, 3, \quad (1)$$

$$\hat{\rho} \hat{u}_{itt} - \hat{C}_{ijkl} \frac{\partial^2 \hat{u}_l}{\partial x_j \partial x_k} = 0, \quad i = 1, 2, 3, \quad (2)$$

where  $u_i$  and  $\hat{u}_i$ ,  $i = 1, 2, 3$ , are components of the displacement vectors. A plain wave propagating in the structure in  $x_1$  direction is of the form:

$$u_i(x_1, x_3) = a_i(x_3) \cos(kx_1 - \omega t) + b_i(x_3) \sin(kx_1 - \omega t), \quad (3)$$

$$\hat{u}_i(x_1, x_3) = \hat{a}_i(x_3) \cos(kx_1 - \omega t) + \hat{b}_i(x_3) \sin(kx_1 - \omega t). \quad (4)$$

Here,  $k$  is the wave value,  $\omega$  the circuit frequency. The substitution of (3) and (4) into (1) and (2), respectively, yields

$$\begin{aligned} -C_{i33l} \ddot{a}_l - (C_{i13l} + C_{i31l}) \dot{b}_l + C_{i11l} a_l - \rho \frac{\omega^2}{k^2} a_i &= 0, \\ -C_{i33l} \ddot{b}_l + (C_{i13l} + C_{i31l}) \dot{a}_l + C_{i11l} b_l - \rho \frac{\omega^2}{k^2} b_i &= 0, \end{aligned}$$

and

$$\begin{aligned} -\hat{C}_{i33l} \ddot{\hat{a}}_l - (\hat{C}_{i13l} + \hat{C}_{i31l}) \dot{\hat{b}}_l + \hat{C}_{i11l} \hat{a}_l - \hat{\rho} \frac{\omega^2}{k^2} \hat{a}_i &= 0, \\ -\hat{C}_{i33l} \ddot{\hat{b}}_l + (\hat{C}_{i13l} + \hat{C}_{i31l}) \dot{\hat{a}}_l + \hat{C}_{i11l} \hat{b}_l - \hat{\rho} \frac{\omega^2}{k^2} \hat{b}_i &= 0, \end{aligned}$$

$i = 1, 2, 3$ .

Here, the dot denotes the differentiation with respect to the variable  $\tilde{x}_3 = kx_3$ . With the state vectors

$$\vec{p} = (a_1, a_2, a_3, b_1, b_2, b_3, \dot{a}_1, \dot{a}_2, \dot{a}_3, \dot{b}_1, \dot{b}_2, \dot{b}_3)^T \in R^{12},$$

$$\hat{\vec{p}} = (\hat{a}_1, \hat{a}_2, \hat{a}_3, \hat{b}_1, \hat{b}_2, \hat{b}_3, \dot{\hat{a}}_1, \dot{\hat{a}}_2, \dot{\hat{a}}_3, \dot{\hat{b}}_1, \dot{\hat{b}}_2, \dot{\hat{b}}_3)^T \in R^{12},$$

the above systems can be rewritten in the normal form as follows:

$$\dot{\vec{p}} = A\vec{p}, \quad \dot{\hat{\vec{p}}} = \hat{A}\hat{\vec{p}}, \quad (5)$$

where  $A$  and  $\hat{A}$  are the corresponding matrices. Let  $\lambda_1, \lambda_2, \dots, \lambda_{12}$  and  $\vec{h}_1, \vec{h}_2, \dots, \vec{h}_{12}$  (respectively,  $\hat{\lambda}_1, \hat{\lambda}_2, \dots, \hat{\lambda}_{12}$  and  $\hat{\vec{h}}_1, \hat{\vec{h}}_2, \dots, \hat{\vec{h}}_{12}$ ) be eigenvalues and eigenvectors of  $A$  (respectively,  $\hat{A}$ ). One can verify that just  $\ell$  linear independent eigenvectors can be found for each  $\ell$ -multiple eigenvalue. Therefore, solutions of (5) are of the form:

$\vec{p}(x_3) = \sum_{i=1}^{12} D_i \vec{h}_i e^{\lambda_i k x_3}$ ,  $\hat{\vec{p}}(x_3) = \sum_{i=1}^{12} \hat{D}_i \hat{\vec{h}}_i e^{\hat{\lambda}_i k x_3}$ , where  $D_i$  and  $\hat{D}_i$  are arbitrary constants. Selecting decreasing solutions in the substrate yields:

$$\vec{p}(x_3) = \sum_{j=1}^N D_j \vec{h}_{i_j} e^{\lambda_{i_j} k x_3}, \quad \text{Re } \lambda_{i_j} > 0.$$

Note that  $N \leq 6$  due to the up-down symmetry of the substrate. Solutions in the upper layer have to be of the oscillatory type:

$$\hat{\vec{p}}(x_3) = \sum_{j=1}^L \hat{D}_j \hat{\vec{h}}_{i_j} e^{\hat{\lambda}_{i_j} k x_3}, \quad \text{Re } \hat{\lambda}_{i_j} = 0.$$

Thus,

$$a_l = \sum_{j=1}^N D_j h_{i_j}^{(l)} e^{\lambda_{i_j} k x_3}, \quad b_l = \sum_{j=1}^N D_j h_{i_j}^{(l+3)} e^{\lambda_{i_j} k x_3},$$

$$\hat{a}_l = \sum_{j=1}^L \hat{D}_j \hat{h}_{i_j}^{(l)} e^{\hat{\lambda}_{i_j} k x_3}, \quad \hat{b}_l = \sum_{j=1}^L \hat{D}_j \hat{h}_{i_j}^{(l+3)} e^{\hat{\lambda}_{i_j} k x_3},$$

where  $l$  runs from 1 to 3. Therefore, the displacements  $u_i$  and  $\hat{u}_i$ , see (3) and (4), depend linearly on  $D_j, j = 1, N$ , and  $\hat{D}_l, l = 1, L$ , respectively.

For all  $x_1$  and  $t$ , the following interface conditions must hold:

$$u_i = \hat{u}_i, \quad \text{at } x_3 = 0, \quad \text{continuity}; \quad (6)$$

$$C_{i3kl} \frac{\partial u_i}{\partial x_k} = \hat{C}_{i3kl} \frac{\partial \hat{u}_i}{\partial x_k}, \quad \text{at } x_3 = 0, \quad \text{equilibrium of pressures}; \quad (7)$$

$$\hat{C}_{i3kl} \frac{\partial \hat{u}_i}{\partial x_k} = 0, \quad \text{at } x_3 = h, \quad \text{free of forces boundary}. \quad (8)$$

The above system yields 18 linear equations for  $N + L \leq 18$  coefficients  $D_j$  and  $\hat{D}_l$ . Note that  $N + L < 18$  as a rule. Let  $V = \omega/k$  be the unknown wave velocity and  $G(V)$  the  $18 \times (N + L)$ -matrix of the above system. Feasible wave velocities are determined from the condition of nontrivial solvability for the system  $G(V)\vec{D} = 0$ , where  $\vec{D} = (D_1, \dots, D_N, \hat{D}_1, \dots, \hat{D}_L)^T$ . Thus, the condition  $\text{rank } G(V) < N + L$  holds for the feasible velocities, which is equivalent to the following condition:  $\det |G^T(V)G(V)| = 0$ . The last equation can be easily solved because the computation of the left-hand-side runs very quickly even on a simple computer. Usually, three roots are being found, which corresponds to three wave types that propagate with different velocities. The selection of the desired wave type is quite obvious because the relation between their velocities is known.

## 2.2 Introducing a fluid

Assume now that the surface of the top layer of the structure shown in Figure 1 contacts with a viscose, weakly compressible fluid. The Stokes equations for compressible viscous fluids read:

$$\rho v_{i,t} - \nu \Delta v_i - (\zeta + \frac{\nu}{3}) \frac{\partial}{\partial x_i} \text{div } v + \frac{\partial}{\partial x_i} p = 0,$$

$$\rho_t + \frac{\partial}{\partial x_i} (\rho v_i) = 0,$$

where  $\rho$  is the density of the fluid,  $v_i, i = 1, 2, 3$ , are components of the velocity field,  $p$  is the static pressure,

$\nu$  and  $\zeta$  are the dynamic and volume viscosities of the fluid, respectively. The weak compressibility means that

$$\varrho(p) \approx \varrho_0 + \alpha \cdot p, \quad \varrho_0 = \varrho(0), \quad \alpha = \frac{\partial \varrho}{\partial p}(0),$$

which yields the following linearized equations:

$$\varrho_0 v_{it} - \nu \Delta v_i - \left(\zeta + \frac{\nu}{3}\right) \frac{\partial}{\partial x_i} \operatorname{div} v + \frac{\partial}{\partial x_i} p = 0, \quad (9)$$

$$\alpha p_t + \varrho_0 \frac{\partial}{\partial x_i} v_i = 0. \quad (10)$$

Just similat to the case of section 2.1, consider plain waves propagating in the fluid in  $x_1$  direction:

$$v_i(x_1, x_3) = c_i(x_3) \cos(kx_1 - \omega t) + d_i(x_3) \sin(kx_1 - \omega t),$$

$$p(x_1, x_3) = e(x_3) \cos(kx_1 - \omega t) + f(x_3) \sin(kx_1 - \omega t).$$

Substituting this ansatz in (9) and (10) results in a system of linear ordinary differential equations for the determination of the amplitudes  $c_i(x_3), d_i(x_3), i = 1, 2, 3, e(x_3)$ , and  $f(x_3)$ . The amplitudes are being represented as linear combinations of exponents with arbitrary coefficients. The matching conditions at the interface between the fluid and the elastic layer consist in the continuity of the velocities and the equilibrium of the normal pressures:

$$v_i = \frac{\partial}{\partial t} \hat{u}_i, \quad (11)$$

$$\hat{C}_{i3kl} \frac{\partial \hat{u}_l}{\partial x_k} = -p \delta_{i3} + \nu \left( \frac{\partial v_i}{\partial x_3} + \frac{\partial v_3}{\partial x_i} \right) + \left(\zeta - \frac{2}{3}\nu\right) \delta_{i3} \operatorname{div} v \quad (12)$$

These relations replace the equation (8) of the system (6)-(7). Then the system (6), (7), (8), (11), (12). is being treated as that is described in section 2.1.

### 2.3 Introducing piezoelectricity

Acoustic waves are usually excited trough piezoelectric materials like crystal  $\alpha$ -quartz. Such materials can transform electric fields into deformations and vice versa so that deformations have influence on themselves trough the electric field. Therefore, the propagation of waves depend on piezoelectric and electric properties of the layers. To explain how the piezoelectric effects can be taken into account, consider a sample structure shown in Figure 2.3.

Because of small deformations, linear constitutive relations for piezoelectric materials are used:

$$\sigma_{ij} = C_{ijkl} \varepsilon_{kl} - e_{kij} E_k$$

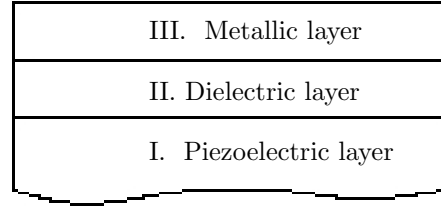


Figure 2: A sample structure consisting of layers with different electric and piezoelectric properties.

$$D_i = \epsilon_{ij} E_j + e_{ikl} \varepsilon_{kl}.$$

Here,  $\sigma_{ij}$  and  $\varepsilon_{kl}$  are the stress and strain tensors, respectively;  $D_i$  and  $E_i$  denote the electric displacement and field, respectively;  $\varepsilon_{kl}$ ,  $e_{kij}$ , and  $C_{ijkl}$  denote the material dielectric tensor, the stress piezoelectric tensor and the elastic stiffness tensor, respectively.

Let  $\phi$  be the potential function such that  $E_i = \frac{\partial \phi}{\partial x_j}$ , then the governing equations derived from the above constitutive relations read:

$$\rho^I u_{itt}^I - C_{ijkl}^I \frac{\partial^2 u_l^I}{\partial x_j \partial x_k} + e_{kij}^I \frac{\partial^2 \phi^I}{\partial x_k \partial x_j} = 0,$$

$$\epsilon_{ij}^I \frac{\partial^2 \phi^I}{\partial x_i \partial x_j} + e_{ikl}^I \frac{\partial^2 u_l^I}{\partial x_i \partial x_k} = 0.$$

For dielectrics without piezoelectric properties, the stress piezoelectric tensor vanishes so that the elasticity equations and the equation determining the potential function are decoupled:

$$\rho^{II} u_{itt}^{II} - C_{ijkl}^{II} \frac{\partial^2 u_l^{II}}{\partial x_j \partial x_k} = 0,$$

$$\epsilon_{ij}^{II} \frac{\partial^2 \phi^{II}}{\partial x_i \partial x_j} = 0$$

Metalls are puerly elastic so that we have

$$\rho^{III} u_{itt}^{III} - C_{ijkl}^{III} \frac{\partial^2 u_l^{III}}{\partial x_j \partial x_k} = 0$$

The conditions on the interface between the piezoelectric, dielectric and metallic layers are the following:

$$C_{i3kl}^I \frac{\partial u_l^I}{\partial x_k} - e_{kij}^I \frac{\partial \phi^I}{\partial x_k} = C_{i3kl}^{II} \frac{\partial u_l^{II}}{\partial x_k}, \quad \text{interface I/II}$$

$$\epsilon_{3j}^I \frac{\partial \phi^I}{\partial x_j} + e_{3kl}^I \frac{\partial u_l^I}{\partial x_k} = \epsilon_{3j}^{II} \frac{\partial \phi^{II}}{\partial x_j}, \quad \text{interface I/II}$$

$$C_{i3kl}^{II} \frac{\partial u_l^{II}}{\partial x_k} = C_{i3kl}^{III} \frac{\partial u_l^{III}}{\partial x_k}, \quad \text{interface II/III}$$

$$\phi^{II} = 0, \quad \text{interface II/III.}$$

The technique described in subsection 2.1 can be applied to treat this case.

### 3 PROGRAM DESCRIPTION

The program is supplied with a user friendly graphical interface written in Visual C++. Using this interface, one can compose a multi-layered structure consisting of arbitrary number of isotropic and anisotropic layers. The material properties such as elastic stiffness tensors can easily be set and edited. If a layer is anisotropic, the orientation of its material is described in terms of successive rotations of the reference system. It is possible to import material parameters from existing models, which is especially convenient when dealing with elastic stiffness tensors containing a lot of coefficients. After composing the structure and specifying the wave frequency, the fitting function is computed and graphically presented (see Fig. 3). Now, the roots of the fitting function can be localized and found precisely along with polarization vectors that indicate the wave types. Moreover, the program possesses an option for the automatic computation of dispersion curves (dependences between the wave velocity and the frequency) for given frequency intervals. Such features make the program useful for researchers working on acoustic sensors.

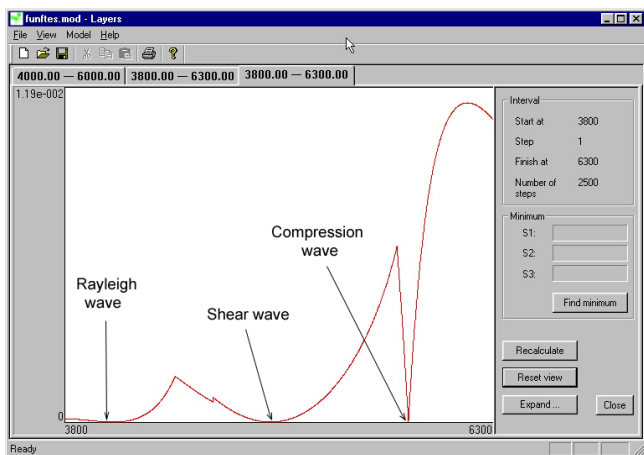


Figure 3: The main window of the program. Roots of the fitting function are the wave velocities for different wave types.

### 4 EXAMPLES

Figure 4 shows the velocity profile for Love shear waves in the structure shown in Figure 1. The substrate is an ST-cut of  $\alpha$ -quartz. The upper layer consists of amorphous quartz. The blank parts of the curve correspond to the absence of Love shear waves for these directions.

Figure 5 shows a dispersion curve generated by the program for a simple structure consisting of a half-space isotropic substrate covered with an isotropic layer. For

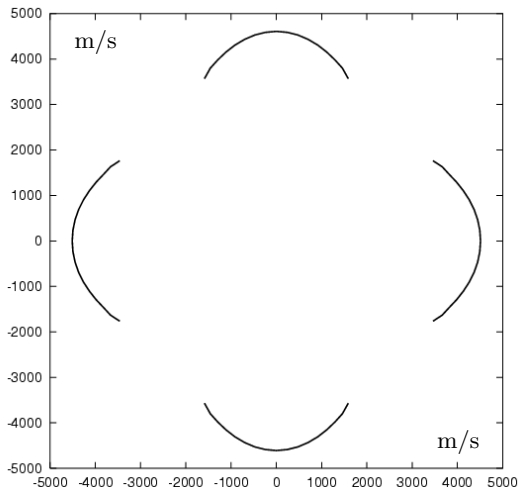


Figure 4: Velocity profile typical for structures with anisotropic substrates possessing rotation symmetries

such a simple structure analytical solution can be found ([2]). The red squares mark points found analytically.

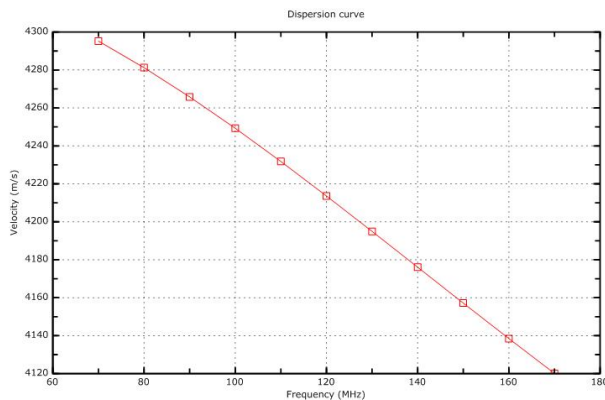


Figure 5: Dispersion curve generated by the program and points found analytically.

Figure 6 demonstrates the application of the method proposed by the authors to the verification of physical experiments related to a biosensor developed at caesar [3]. A 9 nm copper film is deposited on the top layer of the biosensor. Figure 6a shows the time performance of the etching of the copper film. The water flux is being alternated with the flux of an acid solution. The phase shift is being measured. In Figure 6b, the phase shift is computed using dispersion relations. The simulation proves the assumption that the jump at the acid-to-water transition is caused by the change of the fluid viscosity.

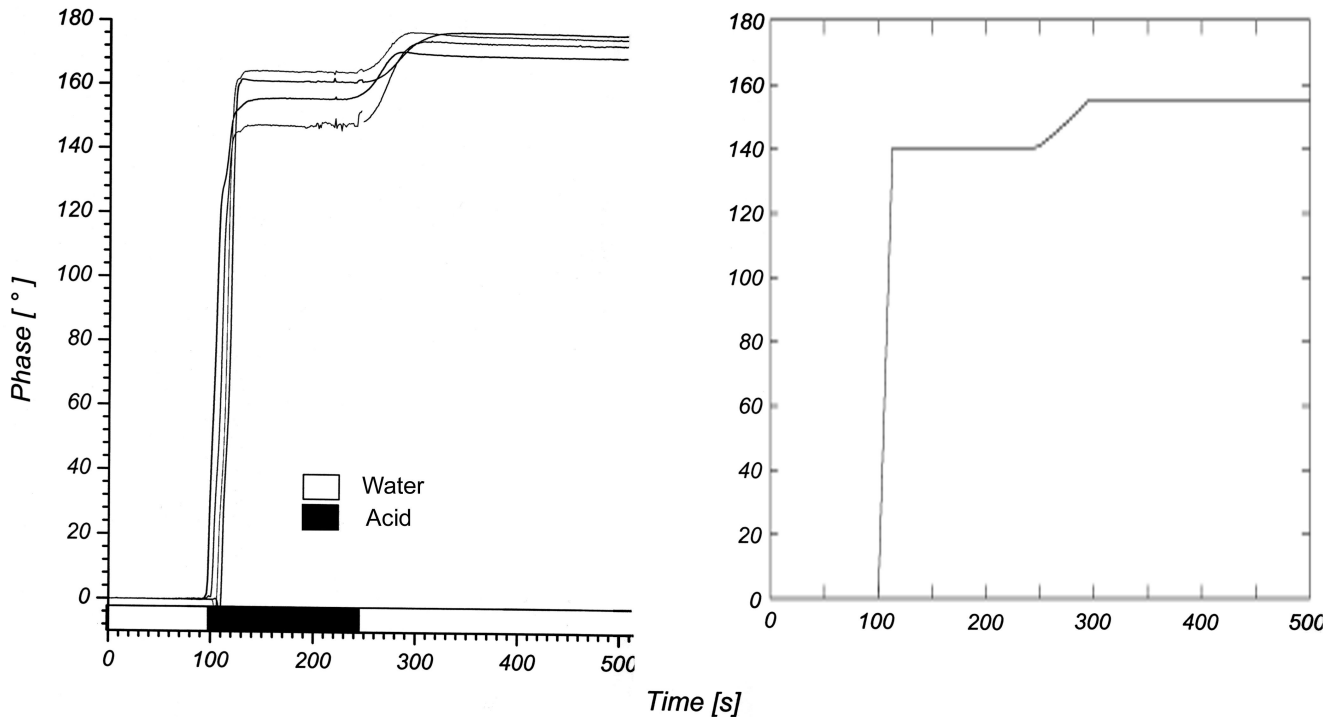


Figure 6: Verification of physical experiments by means of numerical simulations; a: experiment; b: simulation.

## 5 FUTURE WORKS

As that was mentioned in the introduction, the biosensor utilizes adhering of biomolecules to the surface of the top layer which contacts the fluid. Thus, a bristle structure consisting of the biomolecules and moving in the fluid should be introduced in the model. This can be done through the homogenization technique described in [4]. The bristle structure is replaced with an averaged material whose properties are derived as the number of bristles goes to infinity whereas their thickness goes to zero. The computation of parameters of the averaged material will be included into the program.

Sometimes, investigated structures contain very much of periodically alternating layers whose thickness is significantly less than the wave length. Such a sandwich can be replaced by an averaged layer whose properties can be derived by means of the homogenization technique. Note that the homogenization will be performed in the transversal direction only. Therefore, explicit formulas for parameters of the averaged material can be obtained. This option will also be implemented in the program.

## REFERENCES

- [1] N. BOTKIN, M. SCHLENSOG, M. TEWES, AND V. TUROVA, *A mathematical model of a biosensor*, Technical Proceedings of the Fourth International Conference on Modeling and Simulation of Microsystems, 231–234, 2001.
- [2] L.D. LANDAU AND E.M. LIFSCHITZ. *Elastizitätstheorie*, Akademie-Verlag, Berlin, 1975.
- [3] Center of Advanced European Studies and Research, Annual Report 2002 ([www.caesar.de](http://www.caesar.de)).
- [4] N.D. BOTKIN, K.-H. HOFFMANN, V.N. STAROVOITOV, V.L. TUROVA, *Modeling the interaction between bristle elastic structures and fluids*, Proceedings of the 6th International Conference on Modeling and Simulation of Microsystems, February 23–27, 2003, San Francisco, pp. 126–129.

[1] N. BOTKIN, M. SCHLENSOG, M. TEWES, AND